Development of a General Symmetrical Condensed Node for the TLM Method

Vladica Trenkic, *Member, IEEE*, Christos Christopoulos, *Member, IEEE*, and Trevor M. Benson, *Member, IEEE*

Abstract— **A general symmetrical condensed node (GSCN) for the transmission line modeling (TLM) method, with six different link line characteristic impedances, six stubs, and six lossy elements is described for the first time. It unifies all the currently available condensed nodes into a single formulation and provides the basis for the derivation of an infinite set of new nodes, including nodes with improved numerical characteristics. The GSCN is derived in two ways: 1) from an equivalent network model and 2) directly from Maxwell's equations using central differencing and averaging. The direct correspondence established between the GSCN TLM and a finite difference scheme for Maxwell's equations provides a rigorous theoretical foundation for all available TLM methods with condensed nodes.**

I. Introduction

THE SYMMETRICAL condensed node (SCN) [1] has been the basis of the three-dimensional (3-D) transmission line modeling (TLM) method for many years. To allow for the modeling of general lossless materials and nonuniform grading of the mesh cells, the basic 12-port SCN is augmented by three open- and three short-circuit stubs [1]. In a development of the SCN referred to as the hybrid symmetrical condensed node (HSCN) [2], the characteristic impedances of the link lines are varied to account for mesh grading and to model magnetic properties of the mesh, and three open-circuit stubs are used to make up for any deficit in the capacitance. A complementary HSCN, denoted as the Type II HSCN [3], was recently developed using different link-line impedances to model electric properties and short-circuit stubs to correct for any deficit in inductance. In a further recent development of the SCN, referred to as the symmetrical super-condensed node (SSCN) [4]–[6], stubs are removed all together and all medium parameters are modeled by varying the characteristic impedances of the link lines. Modifications of the SCN to account for electric and magnetic losses are described in [7] and [8] and can be readily applied to all other condensed nodes.

In this paper, we present the development of a general symmetrical condensed node (GSCN) that unifies all of the existing condensed node schemes [1]–[8] into a single scheme and provides a template for the derivation of new nodes with improved propagation properties. A general formulation of the link and stub parameters is presented in Section II that can be used in connection with any TLM node. These parameters are determined by a set of 12 equations that ensure proper modeling of the capacitance and inductance of the medium and preservation of impulse synchronism. In Section III-A, the scattering matrix for the GSCN is derived from the equivalent network model [9], [10], which formulates scattering in a node having six different link-line impedances, three open-circuit stubs, three short-circuit stubs, and six lossy elements for modeling electric and magnetic losses. Applying particular constraints to the GSCN, the scattering matrices for all existing condensed nodes [1]–[8] and their parameters are derived from the formulation of the GSCN presented here.

A formal equivalence between the SCN TLM and the time-domain finite-difference (FD-TD) method was first established in [11]. Recently, it was shown that the SCN TLM can be derived directly from Maxwell's equations applying the Method of Moments (MoM) [12]. The two above references, however, consider only the simple 12-port SCN, which cannot model inhomogeneous and lossy media and is restricted only to the cubic cells. More practical schemes, namely the stub-loaded SCN and the HSCN, were only very recently derived directly from Maxwell's equations, using central differencing and averaging [13]. A direct theoretical derivation of the Type II HSCN and the SSCN has not been presented in the literature so far.

In Section III-B, we derive the GSCN directly from Maxwell's equations, using principles established in [13]. This derivation gives the same results for the field components in the GSCN as obtained using the network model in Section III-A, thus offering further evidence of the soundness of the method. Since the symmetrical super-condensed node is derived from the GSCN by removing stubs, a field-based theoretical foundation to the SSCN is also established for the first time.

II. General TLM Constitutive Relations

The total capacitance and inductance of the block of space with linear dimensions $\Delta x, \Delta y, \Delta z$ and material properties $\overline{\overline{\varepsilon}}, \overline{\overline{\mu}}$ defined as diagonal tensors

$$\overline{\overline{\varepsilon}} = \varepsilon_0 \begin{bmatrix} \varepsilon_{rx} & 0 & 0 \\ 0 & \varepsilon_{ry} & 0 \\ 0 & 0 & \varepsilon_{rz} \end{bmatrix} \quad \overline{\overline{\mu}} = \mu_0 \begin{bmatrix} \mu_{rx} & 0 & 0 \\ 0 & \mu_{ry} & 0 \\ 0 & 0 & \mu_{rz} \end{bmatrix} \tag{1}$$

modeled by a TLM node, in the i direction are given as [14]

$$C_t^i = \varepsilon_0 \varepsilon_{ri} \frac{\Delta j \Delta k}{\Delta i} \quad L_t^i = \mu_0 \mu_{ri} \frac{\Delta j \Delta k}{\Delta i} \tag{2}$$

where $i, j, k \in \{x, y, z\}$ and $i \neq j, k$. Equations (2) must hold for any TLM node, constructed by an arbitrary combination

Manuscript received June 10, 1995; revised August 26, 1996. This work was supported in part by the Engineering and Physical Sciences Research Council, U.K.

The authors are with the Department of Electrical and Electronic Engineering, University of Nottingham, NG7 2RD Nottingham, U.K.

Publisher Item Identifier S 0018-9480(96)08478-5.

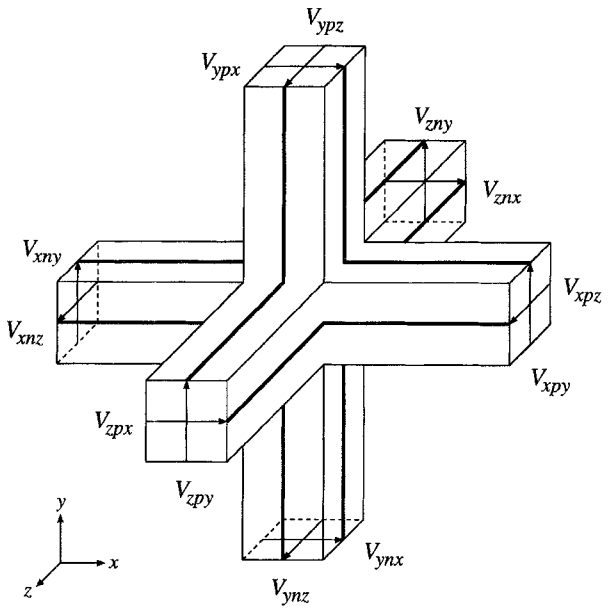

Fig. 1. 3-D TLM symmetrical condensed node (SCN).

of link lines and stubs, and we refer to them as the general TLM constitutive relations.

Consider the TLM symmetrical condensed node depicted in Fig. 1. Let the distributed capacitance and inductance of an i-directed, j-polarized link line be denoted by indexes according to their direction and polarization as C_{ij} and L_{ij}. The total capacitance of an open-circuit stub and the total inductance of a short-circuit stub, contributing to the cell's capacitance and inductance, respectively, in the i direction, are denoted as C_o^i and L_s^i. The general TLM constitutive relations (2) applied to the condensed node can be written as

$$C_{ki}\Delta k + C_{ji}\Delta j + C_o^i = \varepsilon_0\varepsilon_{ri}\frac{\Delta j\Delta k}{\Delta i} \tag{3}$$

$$L_{jk}\Delta j + L_{kj}\Delta k + L_s^i = \mu_0\mu_{ri}\frac{\Delta j\Delta k}{\Delta i}. \tag{4}$$

The six equations defined in (3) and (4) by using all possible combinations of $i, j, k \in \{x, y, z\}$, represent the basis for the correct modeling of the medium using a generally graded TLM mesh with condensed nodes. They contain eighteen unknown parameters, namely C_{ij} and L_{ij} of the six link lines, C_o^i of the three open-circuit stubs, and L_s^i of the three short-circuit stubs. Therefore, there are 12 degrees of freedom that can be specified in the formulation of particular types of symmetrical condensed nodes.

In time-domain TLM schemes, time synchronism must be maintained in the mesh, i.e., the time step Δt must be the same throughout and therefore six more conditions are imposed in the form [5]

$$\Delta t = \Delta i\sqrt{C_{ij}L_{ij}}. \tag{5}$$

With these extra conditions, six degrees of freedom still remain when solving (3)–(5).

It can be readily shown that the link line and stub parameters of the existing 3-D time-domain condensed nodes can be obtained by imposing different constraints to (3)–(5). Based on these restrictions, we give a brief classification of the 3-D TLM condensed nodes used in the time-domain schemes.

1) *Stub-loaded nodes* use the same characteristic impedance for all link lines, which sets six constraints of the form $L_{ij}/C_{ij} = \text{const}$.
2) *Hybrid nodes* use either open or short circuit stubs, so that three extra conditions are given by $L_s^i = 0$ or $C_o^i = 0$. The other three conditions are obtained by demanding that all the impedances of lines modeling either the same magnetic [2] or the same electric [3] field components are equal.
3) *Super-condensed nodes* do not use stubs at all, therefore six extra conditions are given by $C_o^i = 0$ and $L_s^i = 0$ [6].
4) *General nodes* use a combination of the link line and stub parameters in a manner that generally differs from the previous three special cases.

In order to formulate the scattering procedure, the characteristic admittances/impedances of the link and stub lines must be determined, and they are defined as [15]

$$Y_{ij} = \frac{1}{Z_{ij}} = \sqrt{\frac{C_{ij}}{L_{ij}}} \quad Y_{oi} = \frac{2C_o^i}{\Delta t} \quad Z_{si} = \frac{2L_s^i}{\Delta t} \tag{6}$$

where Y_{ij}, Z_{ij} are the characteristic admittance/impedance of an i-directed j-polarized link line and Y_{oi}, Z_{si} are the admittance/impedance of the open-/short-circuit stubs contributing the capacitance/inductance in the i direction. Using the time synchronism condition (5) and definitions of the characteristic admittances/impedances of the link and stub lines (6), the general constitutive relations (3) and (4) can be rewritten as

$$Y_{ki} + Y_{ji} + \frac{Y_{oi}}{2} = \varepsilon_0\varepsilon_{ri}\frac{\Delta j\Delta k}{\Delta i\Delta t} \tag{7}$$

$$Z_{jk} + Z_{kj} + \frac{Z_{si}}{2} = \mu_0\mu_{ri}\frac{\Delta j\Delta k}{\Delta i\Delta t}. \tag{8}$$

In time-domain TLM, losses are modeled by introducing matched stubs, loaded to the nodes at the scattering points [16]. Their presence does not affect the general system of (3)–(5). Given the effective electric and magnetic conductivities σ_{ei} and σ_{mi} in the i direction, the parameters of lossy elements are defined as [7], [8]

$$G_{ei} = \sigma_{ei}\frac{\Delta j\Delta k}{\Delta i} \quad R_{mi} = \sigma_{mi}\frac{\Delta j\Delta k}{\Delta i}. \tag{9}$$

III. General Symmetrical Condensed Node

It can be seen from the TLM constitutive relations (3) and (4) that the contributions to the capacitance and the inductance required in a model can be divided between the link lines and stubs of a TLM node. Theoretically, it is possible to develop a general condensed node that will contain six stubs, six lossy elements, and have all six link lines with different characteristic impedance. The merit of this formulation is that it offers scope for optimization by selecting a particular combination of stubs and link line parameters, which, however, must satisfy (7) and (8). The properties of the general symmetrical condensed node (GSCN) are obtained below using two different approaches, namely: 1) an equivalent network

$\mathbf{S} =$

	1	2	3	4	5	6	7	8	9	10	11	12	13	14	15	16	17	18
1	a_{yx}	b_{yx}	d_{yx}	0	0	0	0	0	b_{yx}	0	$-d_{yx}$	c_{yx}	g_x	0	0	0	0	i_{yx}
2	b_{zx}	a_{zx}	0	0	0	d_{zx}	0	0	c_{zx}	$-d_{zx}$	0	b_{zx}	g_x	0	0	0	$-i_{zx}$	0
3	d_{xy}	0	a_{xy}	b_{xy}	0	0	0	b_{xy}	0	0	c_{xy}	$-d_{xy}$	0	g_y	0	0	0	$-i_{xy}$
4	0	0	b_{zy}	a_{zy}	d_{zy}	0	$-d_{zy}$	c_{zy}	0	0	b_{zy}	0	0	g_y	0	i_{zy}	0	0
5	0	0	0	d_{yz}	a_{yz}	b_{yz}	c_{yz}	$-d_{yz}$	0	b_{yz}	0	0	0	0	g_z	$-i_{yz}$	0	0
6	0	d_{xz}	0	0	b_{xz}	a_{xz}	b_{xz}	0	$-d_{xz}$	c_{xz}	0	0	0	0	g_z	0	i_{xz}	0
7	0	0	0	$-d_{yz}$	c_{yz}	b_{yz}	a_{yz}	d_{yz}	0	b_{yz}	0	0	0	0	g_z	i_{yz}	0	0
8	0	0	b_{zy}	c_{zy}	$-d_{zy}$	0	d_{zy}	a_{zy}	0	0	b_{zy}	0	0	g_y	0	$-i_{zy}$	0	0
9	b_{zx}	c_{zx}	0	0	0	$-d_{zx}$	0	0	a_{zx}	d_{zx}	0	b_{zx}	g_x	0	0	0	i_{zx}	0
10	0	$-d_{xz}$	0	0	b_{xz}	c_{xz}	b_{xz}	0	d_{xz}	a_{xz}	0	0	0	0	g_z	0	$-i_{xz}$	0
11	$-d_{xy}$	0	c_{xy}	b_{xy}	0	0	0	b_{xy}	0	0	a_{xy}	d_{xy}	0	g_y	0	0	0	i_{xy}
12	c_{yx}	b_{yx}	$-d_{yx}$	0	0	0	0	0	b_{yx}	0	d_{yx}	a_{yx}	g_x	0	0	0	0	$-i_{yx}$
13	e_{yx}	e_{zx}	0	0	0	0	0	0	e_{zx}	0	0	e_{yx}	h_x	0	0	0	0	0
14	0	0	e_{xy}	e_{zy}	0	0	0	e_{zy}	0	0	e_{xy}	0	0	h_y	0	0	0	0
15	0	0	0	0	e_{yz}	e_{xz}	e_{yz}	0	0	e_{xz}	0	0	0	0	h_z	0	0	0
16	0	0	0	f_x	$-f_x$	0	f_x	$-f_x$	0	0	0	0	0	0	0	j_x	0	0
17	0	$-f_y$	0	0	0	f_y	0	0	f_y	$-f_y$	0	0	0	0	0	0	j_y	0
18	f_z	0	$-f_z$	0	0	0	0	0	0	0	f_z	$-f_z$	0	0	0	0	0	j_z
19	k_{yx}	k_{zx}	0	0	0	0	0	0	k_{zx}	0	0	k_{yx}	l_x	0	0	0	0	0
20	0	0	k_{xy}	k_{zy}	0	0	0	k_{zy}	0	0	k_{xy}	0	0	l_y	0	0	0	0
21	0	0	0	0	k_{yz}	k_{xz}	k_{yz}	0	0	k_{xz}	0	0	0	0	l_z	0	0	0
22	0	0	0	m_x	$-m_x$	0	m_x	$-m_x$	0	0	0	0	0	0	0	n_x	0	0
23	0	$-m_y$	0	0	0	m_y	0	0	m_y	$-m_y$	0	0	0	0	0	0	n_y	0
24	m_z	0	$-m_z$	0	0	0	0	0	0	0	m_z	$-m_z$	0	0	0	0	0	n_z

Fig. 2. Scattering matrix of the general symmetrical condensed node (GSCN). (The first row and column are not part of the matrix. They give the port numbering for convenience.)

model and 2) central differencing and averaging of Maxwell's equations.

A. Derivation from the Network Model

Scattering in a condensed node scheme is traditionally derived by imposing unitary and other conditions on its scattering matrix [1]. However, a network model introduced in [9] and generalized and validated in [10] shows that scattering in condensed nodes can be conveniently described by scattering equations derived directly from the set of "equivalent" shunt and series circuits. For historical reasons and in order to allow comparisons with previous nodes, we also present the complete scattering matrix for the GSCN. For the same reasons, we keep the original node port numbering scheme [1], [15], although more elegant numbering schemes described recently [17], [18] yield a more symmetrical form of the scattering matrix.

In the notation used here a voltage coming from the negative side of the node (assuming the origin of coordinates at the center of the node) along an i-directed, j-polarized transmission line is denoted as V_{inj}, whereas a voltage coming from the positive side of the same line is given as V_{ipj} ($i,j \in \{x,y,z\}$ and $i \neq j$). Voltages on the open- and short-circuit stubs are V_{oi} and V_{si}, whereas the voltages on electric and magnetic loss elements are V_{ei} and V_{mi}. In all cases, voltages incident on the node have superscript i while reflected voltages have superscript r.

By following the principles established in [9] and [10], the complete scattering procedure in the GSCN can be described by the following equations:

$$V_{inj}^r = V_j \pm I_k Z_{ij} - V_{ipj}^i \tag{10}$$

$$V_{ipj}^r = V_j \mp I_k Z_{ij} - V_{inj}^i \tag{11}$$

where the upper and lower signs apply, respectively, for indexes $(i,j,k) \in \{(x,y,z),(y,z,x),(z,x,y)\}$ and $(i,j,k) \in \{(x,z,y),(y,x,z),(z,y,x)\}$. The equivalent voltage in the i direction, V_i, is given by

$$V_i = \frac{2Y_{ki}(V_{kni}^i + V_{kpi}^i) + 2Y_{ji}(V_{jni}^i + V_{jpi}^i) + 2Y_{oi}V_{oi}^i}{2(Y_{ki} + Y_{ji}) + Y_{oi} + G_{ei}} \tag{12}$$

and the equivalent current contributing to the magnetic field in the i direction, I_i, is given by

$$I_i = \frac{2(V_{jpk}^i - V_{jnk}^i + V_{knj}^i - V_{kpj}^i - V_{si}^i)}{2(Z_{jk} + Z_{kj}) + Z_{si} + R_{mi}} \tag{13}$$

where $(i,j,k) \in \{(x,y,z),(y,z,x),(z,x,y)\}$. The voltages reflected to stubs and lossy elements are given as

$$V_{oi}^r = V_i - V_{oi}^i \tag{14}$$

$$V_{si}^r = I_i Z_{si} + V_{si}^i \tag{15}$$

$$V_{ei}^r = V_i \tag{16}$$

$$V_{mi}^r = R_{mi} I_i \tag{17}$$

where $i \in \{x,y,z\}$.

Using the scattering equations (10)–(17), we obtain the scattering matrix for the GSCN, given in Fig. 2. Because there are no incident voltages from lossy elements, the matrix $\boldsymbol{S}$ is written as a 24 × 18 matrix rather then a full 24 × 24 square matrix with zero columns 19–24. The elements of the scattering matrix $\boldsymbol{S}$ shown in Fig. 2 are

$$\begin{aligned}
a_{ij} &= Q_j - b_{ij} - d_{ij} & b_{ij} &= Q_j \hat{C}_{kj} \\
c_{ij} &= Q_j - b_{ij} + d_{ij} - 1 & d_{ij} &= P_k \hat{L}_{ij} \\
f_k &= 2(1 - P_k - U_k) & e_{ij} &= b_{kj} \\
g_j &= 2(1 - Q_j - W_j) & i_{ij} &= d_{ij} \\
h_j &= g_j - 1 & j_k &= 1 - f_k \\
k_{ij} &= e_{ij} & l_j &= g_j \\
m_k &= 2U_k & n_k &= -m_k
\end{aligned} \tag{18}$$

with

$$\hat{C}_{kj} = \frac{Y_{kj}}{Y_{ij} + Y_{kj}} = \frac{Z_{ij}}{Z_{ij} + Z_{kj}} \tag{19}$$

$$\hat{L}_{ij} = \frac{Z_{ij}}{Z_{ij} + Z_{ji}} \tag{20}$$

$$Q_j = \left(1 + \frac{Y_{oj} + G_{ej}}{2(Y_{ij} + Y_{kj})}\right)^{-1} \tag{21}$$

$$P_k = \left(1 + \frac{Z_{sk} + R_{mk}}{2(Z_{ij} + Z_{ji})}\right)^{-1} \tag{22}$$

$$W_j = \frac{G_{ej}}{2(Y_{ij} + Y_{kj}) + Y_{oj} + G_{ej}} \tag{23}$$

$$U_k = \frac{R_{mk}}{2(Z_{ij} + Z_{ji}) + Z_{sk} + R_{mk}} \tag{24}$$

where indexes i, j, k take all possible combinations of x, y, z.

The matrix $\boldsymbol{S}$ can be written in the following partitioned form, where each submatrix represents one of the matrices outlined in Fig. 2

$$\boldsymbol{S} = \begin{bmatrix} \boldsymbol{S}_{ln}^{(12\times12)} & \boldsymbol{S}_{os\to ln}^{(12\times3)} & \boldsymbol{S}_{ss\to ln}^{(12\times3)} \\ \boldsymbol{S}_{ln\to os}^{(3\times12)} & \boldsymbol{S}_{os}^{(3\times3)} & \boldsymbol{0}^{(3\times3)} \\ \boldsymbol{S}_{ln\to ss}^{(3\times12)} & \boldsymbol{0}^{(3\times3)} & \boldsymbol{S}_{ss}^{(3\times3)} \\ \boldsymbol{S}_{ln\to el}^{(3\times12)} & \boldsymbol{S}_{os\to el}^{(3\times3)} & \boldsymbol{0}^{(3\times3)} \\ \boldsymbol{S}_{ln\to ml}^{(3\times12)} & \boldsymbol{0}^{(3\times3)} & \boldsymbol{S}_{ss\to ml}^{(3\times3)} \end{bmatrix}. \tag{25}$$

The indexes ln, os, ss, el, ml, indicating the physical purpose of each submatrix, stand for link line, open-circuit stub, short-circuit stub, electric loss, and magnetic loss voltage ports, respectively. The superscripts of the submatrices define their size. Some partitions can be removed from the matrix if stubs or lossy elements are not used. For example, if short-circuit stubs and lossy elements are not used in the node, all partitions with indexes ss, el and ml can be removed from $\boldsymbol{S}$ giving a 15×15 matrix.

By removing lossy elements from the node, setting $G_{ej} = 0$ and $R_{mk} = 0$ in (21)–(24) and eliminating rows 19–24 in the scattering matrix $\boldsymbol{S}$, it can be shown that the lossless GSCN conserves energy by confirming that $\boldsymbol{S}^T\boldsymbol{Y}\boldsymbol{S} = \boldsymbol{Y}$ [19], where $\boldsymbol{Y}$ is a diagonal matrix with elements corresponding to the characteristic admittances of link lines and stubs.

The matrix $\boldsymbol{S}$ has identical structure to the scattering matrix for the stub-loaded SCN [15]. By setting the characteristic impedances of link lines equal to the intrinsic impedance of the background medium, i.e., letting $Z_{ij} = Z_0$, the elements of the GSCN and the SCN scattering matrix become equal, as expected. If an homogeneous lossless medium is modeled on a uniform mesh, then stubs and lossy elements can be eliminated by setting $Y_{oj} = Z_{sk} = G_{ej} = R_{mk} = 0$ in (21)–(24) and the partition $\boldsymbol{S}_{ln}$ of the matrix $\boldsymbol{S}$ becomes equal to the original 12-port SCN matrix [1] with the elements $a_{ij} = c_{ij} = 0$ and $b_{ij} = d_{ij} = 1/2$.

Similarly, by setting $Z_{ij} = Z_{ji}$ and $Z_{sk} = 0$, for all combinations of indexes $i, j, k \in \{x, y, z\}$, $i \neq j, k$ and eliminating partitions of $\boldsymbol{S}$ related to the short-circuit stubs, the scattering matrix of the HSCN [2], [3] is derived. The scattering matrix for the Type II HSCN [3] can be derived from $\boldsymbol{S}$ by setting $Y_{ij} = Y_{kj}, Y_{oj} = 0$ and eliminating the partitions related to the open-circuit stubs.

The scattering matrix for the SSCN is derived from the GSCN by eliminating row/columns 13–18 of $\boldsymbol{S}$ and setting $Y_{oj} = Z_{sk} = 0$. If a lossless medium is modeled, then the SSCN scattering matrix is defined by the submatrix $\boldsymbol{S}_{ln}$, with elements $a_{ij} = 1 - b_{ij} - d_{ij}$, $c_{ij} = d_{ij} - b_{ij}$, $b_{ij} = \hat{C}_{ik}$ and $d_{ij} = \hat{L}_{ij}$, as derived in [6]. This matrix applies also for frequency-domain TLM schemes with different line impedances [20], [21].

B. Derivation from Maxwell's Equations

We now derive the GSCN TLM scheme directly from Maxwell's equations, by employing a procedure similar to that used in [13]. Maxwell's equations, written in the Cartesian coordinate system, are given as

$$\begin{aligned} \varepsilon_0\varepsilon_{ri}\frac{\partial E_i}{\partial t} &= \frac{\partial H_k}{\partial j} - \frac{\partial H_j}{\partial k} - \sigma_{ei}E_i \\ \mu_0\mu_{ri}\frac{\partial H_i}{\partial t} &= \frac{\partial E_j}{\partial k} - \frac{\partial E_k}{\partial j} - \sigma_{mi}H_i. \end{aligned} \tag{26}$$

Six equations are contained in (26) if the mapping of indexes is introduced as

$$(i, j, k) \in \{(x, y, z), (y, z, x), (z, x, y)\}. \tag{27}$$

The mapping given by (27) will be used throughout this subsection. It allows the rotation of dummy indexes i, j, k in an arbitrary expression F, making the expressions $F(i, j, k), F(j, k, i)$ and $F(k, i, j)$ equivalent.

After performing coordinate and field transformations given by

$$\begin{aligned} k &= \hat{k}\Delta k; \quad t = \hat{t}\Delta t \\ E_k &= -V_k/\Delta k; \quad H_k = I_k/\Delta k \end{aligned} \tag{28}$$

where $k \in \{x, y, z\}$, Maxwell's equations (26) can be rewritten as

$$\begin{aligned} \varepsilon_0\varepsilon_{ri}\frac{\Delta j\Delta k}{\Delta i\Delta t}\frac{\partial V_i}{\partial \hat{t}} &= \frac{\partial I_j}{\partial \hat{k}} - \frac{\partial I_k}{\partial \hat{j}} - \sigma_{ei}\frac{\Delta j\Delta k}{\Delta i}V_i \\ \mu_0\mu_{ri}\frac{\Delta j\Delta k}{\Delta i\Delta t}\frac{\partial I_i}{\partial \hat{t}} &= \frac{\partial V_k}{\partial \hat{j}} - \frac{\partial V_j}{\partial \hat{k}} - \sigma_{mi}\frac{\Delta j\Delta k}{\Delta i}I_i. \end{aligned} \tag{29}$$

By further inserting (7)–(9) into (29), we obtain

$$\begin{aligned} \left(Y_{ki} + Y_{ji} + \frac{Y_{oi}}{2}\right)\frac{\partial V_i}{\partial \hat{t}} &= \frac{\partial I_j}{\partial \hat{k}} - \frac{\partial I_k}{\partial \hat{j}} - G_{ei}V_i \\ \left(Z_{jk} + Z_{kj} + \frac{Z_{si}}{2}\right)\frac{\partial I_i}{\partial \hat{t}} &= \frac{\partial V_k}{\partial \hat{j}} - \frac{\partial V_j}{\partial \hat{k}} - R_{mi}I_i. \end{aligned} \tag{30}$$

In this formulation, Y, Z, G, and R can be formally considered as coefficients introduced into Maxwell's equations to conveniently represent material parameters and cell dimensions. They are chosen in a manner to allow for sufficient degrees of freedom demanded by the GSCN. However, through (7)–(9), these coefficients have the physical interpretation as

the link and stub admittances/impedances of the GSCN. In the derivation of the SCN presented in [12] these coefficients were not explicitly introduced since there were no stubs and all the link-line impedances were identical.

Following [13] we introduce mixed space-time coordinates as

$$\xi_k = \hat{k} + \hat{t}; \quad \eta_k = \hat{k} - \hat{t}$$

for $k \in \{x, y, z\}$ and rewrite (30) as

$$\begin{aligned}
&\frac{Y_{ki}}{2}\left(\frac{\partial(V_i - I_j Z_{ki})}{\partial \xi_k} - \frac{\partial(V_i + I_j Z_{ki})}{\partial \eta_k}\right) \\
&\quad + \frac{Y_{ji}}{2}\left(\frac{\partial(V_i + I_k Z_{ji})}{\partial \xi_j} - \frac{\partial(V_i - I_k Z_{ji})}{\partial \eta_j}\right) \\
&\quad + \frac{Y_{oi}}{2}\frac{\partial V_i}{\partial \hat{t}} + G_{ei} V_i = 0 \\
&-\frac{1}{2}\left(\frac{\partial(V_k - I_i Z_{jk})}{\partial \xi_j} + \frac{\partial(V_k + I_i Z_{jk})}{\partial \eta_j}\right) \\
&\quad + \frac{1}{2}\left(\frac{\partial(V_j + I_i Z_{kj})}{\partial \xi_k} + \frac{\partial(V_j - I_i Z_{kj})}{\partial \eta_k}\right) \\
&\quad + \frac{Z_{si}}{2}\frac{\partial I_i}{\partial \hat{t}} + R_{mi} I_i = 0. \qquad (31)
\end{aligned}$$

By using central-differencing at point (n, p, q, r) [13], where n is a time and p, q, r are space coordinates, a set of finite difference equations can be obtained from (31). The space coordinates of the cell's boundaries and the cell's center are referred to as

$$(p \pm \tfrac{1}{2}, q, r) = (x^{\pm}) \quad (p, q \pm \tfrac{1}{2}, r) = (y^{\pm})$$
$$(p, q, r \pm \tfrac{1}{2}) = (z^{\pm}) \quad (p, q, r) = (c).$$

The terms associated with the mixed coordinates ξ_k are differenced as, for example

$$\begin{aligned}
\frac{\partial(V_i - I_j Z_{ki})}{\partial \xi_k} &= [{}_{n+(1/2)}V_i(k^+) - {}_{n+(1/2)}I_j(k^+)Z_{ki}] \\
&\quad - [{}_{n-(1/2)}V_i(k^-) - {}_{n-(1/2)}I_j(k^-)Z_{ki}]
\end{aligned}$$

whereas terms associated with η_k are differenced as, for example

$$\begin{aligned}
\frac{\partial(V_i + I_j Z_{ki})}{\partial \eta_k} &= [{}_{n-(1/2)}V_i(k^+) + {}_{n-(1/2)}I_j(k^+)Z_{ki}] \\
&\quad - [{}_{n+(1/2)}V_i(k^-) + {}_{n+(1/2)}I_j(k^-)Z_{ki}].
\end{aligned}$$

The terms associated with the time coordinate $\hat{t}$ are differenced as, for example

$$\frac{\partial V_i}{\partial \hat{t}} = {}_{n+(1/2)}V_i(c) - {}_{n-(1/2)}V_i(c).$$

Similarly as in [13], we now introduce the variable transformation in order to establish relationships between the electric and magnetic field components at the cell boundaries and the incident and reflected voltages at the cell center:

$$\begin{aligned}
{}_{n\mp(1/2)}V_i(k^+) \pm {}_{n\mp(1/2)}I_j(k^+)Z_{ki} &= 2 \cdot {}_nV^{i,r}_{kpi} \\
{}_{n\mp(1/2)}V_i(k^-) \mp {}_{n\mp(1/2)}I_j(k^-)Z_{ki} &= 2 \cdot {}_nV^{i,r}_{kni} \\
{}_{n\mp(1/2)}V_i(j^+) \mp {}_{n\mp(1/2)}I_k(j^+)Z_{ji} &= 2 \cdot {}_nV^{i,r}_{jpi} \\
{}_{n\mp(1/2)}V_i(j^-) \pm {}_{n\mp(1/2)}I_k(j^-)Z_{ji} &= 2 \cdot {}_nV^{i,r}_{jni} \qquad (32)
\end{aligned}$$

where the upper and lower signs, respectively, correspond to the incident and reflected voltages.

A similar transformation which establishes a correspondence between the electrical and magnetic field components at the cell center and the incident and reflected voltages on the open and short stubs is given as

$$\begin{aligned}
{}_{n\mp(1/2)}V_i(c) &= 2 \cdot {}_nV^{i,r}_{oi} \\
{}_{n\mp(1/2)}I_i(c)Z_{si} &= \mp 2 \cdot {}_nV^{i,r}_{si}. \qquad (33)
\end{aligned}$$

By substituting transformations (32) and (33) into difference equations obtained from (31) we derive

$$\begin{aligned}
&Y_{ki} \cdot ({}_nV^i_{kni} + {}_nV^i_{kpi}) + Y_{ji} \cdot ({}_nV^i_{jni} + {}_nV^i_{jpi}) + Y_{oi} \cdot {}_nV^i_{oi} \\
&\quad = Y_{ki} \cdot ({}_nV^r_{kni} + {}_nV^r_{kpi}) + Y_{ji} \cdot ({}_nV^r_{jni} + {}_nV^r_{jpi}) \\
&\quad\quad + Y_{oi} \cdot {}_nV^r_{oi} + G_{ei} \cdot {}_nV_i(c) \qquad (34)
\end{aligned}$$

$$\begin{aligned}
&{}_nV^r_{jnk} - {}_nV^r_{jpk} - {}_nV^r_{knj} + {}_nV^r_{kpj} + {}_nV^r_{si} + R_{mi} \cdot {}_nI_i(c) \\
&\quad = -[{}_nV^i_{jnk} - {}_nV^i_{jpk} - {}_nV^i_{knj} + {}_nV^i_{kpj} + {}_nV^i_{si}]. \qquad (35)
\end{aligned}$$

These two equations represent, respectively, the charge and the flux conservation laws in the i-direction [22].

Another set of finite difference equations can be obtained from (30) by using central differencing at point $(n + 1/2, p, q, r)$

$$\begin{aligned}
&\left(Y_{ki} + Y_{ji} + \frac{Y_{oi}}{2}\right)[{}_{n+1}V_i(c) - {}_nV_i(c)] + G_{ei} \cdot {}_{n+(1/2)}V_i(c) \\
&\quad = [{}_{n+(1/2)}I_j(k^+) - {}_{n+(1/2)}I_j(k^-)] \\
&\quad\quad - [{}_{n+(1/2)}I_k(j^+) - {}_{n+(1/2)}I_k(j^-)] \\
&\left(Z_{jk} + Z_{kj} + \frac{Z_{si}}{2}\right)[{}_{n+1}I_i(c) - {}_nI_i(c)] + R_{mi} \cdot {}_{n+(1/2)}I_i(c) \\
&\quad = [{}_{n+(1/2)}V_k(j^+) - {}_{n+(1/2)}V_k(j^-)] \\
&\quad\quad - [{}_{n+(1/2)}V_j(k^+) - {}_{n+(1/2)}V_j(k^-)]. \qquad (36)
\end{aligned}$$

Terms ${}_{n+(1/2)}V_i(c)$ and ${}_{n+(1/2)}I_i(c)$ can be approximated using central averaging with respect to $\hat{t}$

$$2 \cdot {}_{n+(1/2)}A_i(c) \approx {}_nA_i(c) + {}_{n+1}A_i(c) \quad A \in \{V, I\}. \qquad (37)$$

From transformation (32), the following expressions can be readily obtained:

$$\begin{aligned}
{}_{n+(1/2)}I_j(k^+)Z_{ki} &= {}_{n+1}V^i_{kpi} - {}_nV^r_{kpi} \\
{}_{n+(1/2)}I_j(k^-)Z_{ki} &= -({}_{n+1}V^i_{kni} - {}_nV^r_{kni}) \\
{}_{n+(1/2)}I_k(j^+)Z_{ji} &= -({}_{n+1}V^i_{jpi} - {}_nV^r_{jpi}) \\
{}_{n+(1/2)}I_k(j^-)Z_{ji} &= {}_{n+1}V^i_{jni} - {}_nV^r_{jpi} \\
{}_{n+(1/2)}V_j(k^+) &= {}_{n+1}V^i_{kpj} + {}_nV^r_{kpj} \\
{}_{n+(1/2)}V_j(k^-) &= {}_{n+1}V^i_{knj} + {}_nV^r_{knj} \\
{}_{n+(1/2)}V_k(j^+) &= {}_{n+1}V^i_{jpk} + {}_nV^r_{jpk} \\
{}_{n+(1/2)}V_k(j^-) &= {}_{n+1}V^i_{jnk} + {}_nV^r_{jnk}. \qquad (38)
\end{aligned}$$

From transformation (33) it follows that

$${}_{n+1}V^i_{oi} = {}_nV^r_{oi} \qquad {}_{n+1}V^i_{si} = -{}_nV^r_{si}. \qquad (39)$$

By substituting (37)–(39) into (36) we obtain

$$\left(Y_{k\iota}+Y_{j\iota}+\frac{Y_{o\iota}+G_{e\iota}}{2}\right)[{}_{n+1}V_\iota(c)-{}_nV_\iota(c)]$$
$$=Y_{k\iota}({}_{n+1}V^i_{kn\iota}+{}_{n+1}V^\iota_{kpi})+Y_{j\iota}({}_{n+1}V^\iota_{jn\iota}+{}_{n+1}V^i_{jp\iota})$$
$$+Y_{o\iota}\cdot{}_{n+1}V^\iota_{oi}-[Y_{k\iota}({}_nV^r_{kn\iota}+{}_nV^r_{kp\iota})$$
$$+Y_{j\iota}({}_nV^r_{jn\iota}+{}_nV^r_{jp\iota})$$
$$+Y_{o\iota}\cdot{}_nV^r_{o\iota}+G_{e\iota}\cdot{}_nV_\iota(c)] \tag{40}$$

$$\left(Z_{jk}+Z_{kj}+\frac{Z_{s\iota}+R_{m\iota}}{2}\right)[{}_{n+1}I_\iota(c)-{}_nI_\iota(c)]$$
$$=-[{}_nV^r_{jnk}-{}_nV^r_{jpk}-{}_nV^r_{knj}+{}_nV^r_{kpj}+{}_nV^r_{si}$$
$$+R_{m\iota}\cdot{}_nI_\iota(c)]$$
$$-[{}_{n+1}V^j_{jnk}-{}_{n+1}V^\iota_{jpk}-{}_{n+1}V^\iota_{knj}+{}_{n+1}V^i_{kpj}$$
$$+{}_{n+1}V^\iota_{s\iota}]. \tag{41}$$

Finally, substituting (34) and (35) into (40) and (41) we obtain voltages and currents at the center of the node at time step n as

$$V_\iota(c)=\frac{2Y_{k\iota}(V^\iota_{kni}+V^\iota_{kpi})+2Y_{j\iota}(V^\iota_{jn\iota}+V^\iota_{jpi})+2Y_{o\iota}V^\iota_{oi}}{2(Y_{k\iota}+Y_{ji})+Y_{oi}+G_{e\iota}} \tag{42}$$

$$I_i(c)=\frac{2(V^\iota_{jpk}-V^\iota_{jnk}+V^\iota_{knj}-V^\iota_{kpj}-V^\iota_{s\iota})}{2(Z_{jk}+Z_{kj})+Z_{si}+R_{m\iota}} \tag{43}$$

which are equivalent to (12) and (13) derived from the network model.

The scattering matrix for the GSCN can be derived by averaging appropriate field components at point (n,p,q,r) in the mixed coordinate system. The procedure is similar to that used in [13]. For example, by averaging the component $(V_\iota+I_jZ_{ki})$ with respect to η_k we obtain

$$2[{}_nV_\iota(c)+{}_nI_j(c)Z_{ki}]$$
$$=[{}_{n-(1/2)}V_\iota(k^+)+{}_{n-(1/2)}I_j(k^+)Z_{k\iota}]$$
$$+[{}_{n+(1/2)}V_\iota(k^-)+{}_{n+(1/2)}I_j(k^-)Z_{k\iota}]. \tag{44}$$

Substituting (32) into (44) we derive a reflected voltage at the time step n as

$$V^r_{kni}=V_\iota(c)+I_j(c)Z_{k\iota}-V^\iota_{kp\iota} \tag{45}$$

where $V_\iota(c)$ and $I_j(c)$ are defined from (42) and (43). Similarly, by averaging the component $(V_\iota-I_jZ_{k\iota})$ with respect to ξ_k it can be found that

$$V^r_{kp\iota}=V_\iota(c)-I_j(c)Z_{k\iota}-V^\iota_{kn\iota}. \tag{46}$$

A set of 12 scattering equations for all link lines can be derived in this manner and they are found to be in agreement with the scattering equations (10) and (11) derived from the network model.

Averaging V_ι and I_ι with respect to $\hat{t}$ at the point $(n.p,q,r)$ gives

$$2\cdot{}_nA_\iota(c)={}_{n-(1/2)}A_\iota(c)+{}_{n+(1/2)}A_\iota(c)\quad A\in\{V,I\}$$

which after using (33) gives the voltages reflected to the stubs at the time step n as

$$V^r_{oi}=V_\iota(c)-V^i_{oi}$$
$$V^r_{si}=I_\iota(c)Z_{s\iota}+V^\iota_{si}. \tag{47}$$

These expressions are equivalent to (14) and (15) obtained from the network model.

Because there are no incident voltages from lossy elements, pulses "reflected" to these elements are determined directly from the voltages and currents at the center of the node

$$V^r_{e\iota}=V_\iota(c)\quad V^r_{m\iota}=R_{mi}I_\iota(c). \tag{48}$$

Therefore, the complete set of 24 scattering equations is given by (45)–(48), which is identical to the scattering matrix for the GSCN already derived from the network model and presented in Fig. 2.

IV. Discussion and Conclusions

The formulation of the general symmetrical condensed node given here is derived both from the equivalent network model and from Maxwell's equations. Thus far, it has been shown in [10] that the network model [9] can be derived from a set of decoupled series and shunt circuits by applying the charge and flux conservation law and the continuity of electric and magnetic fields [22]. Here, it has been shown that the scattering equations described by (10)–(17), or equivalently by (45)–(48), can also be established directly from Maxwell's equations (26) by using a mathematical model of central finite differencing and averaging.

It has been shown that the GSCN unifies all available condensed nodes into a single formulation and that all nodes can be derived from the GSCN by imposing appropriate additional conditions to the TLM constitutive relations (3) and (4). The full equivalence established between the GSCN TLM and Maxwell's equations offers a rigorous theoretical foundation to all nodes contained in the formulation of the GSCN. This gives for the first time a field-based formulation of the symmetrical super-condensed node (SSCN), which can be derived from the GSCN by removing all stubs, and provides the theoretical foundation for any new GSCN-based condensed node scheme with an arbitrary number of stubs and different link lines. Following the discussion about accuracy given in [13], one may conclude that all the TLM methods based on the GSCN will have second order accuracy.

The formulation of the GSCN derived from Maxwell's equations gives clear insight into the mapping between the field components and the transmission line voltages in the model. All field components can be obtained from the center of a cell at the time moments $n-1,n,n+1,\cdots$, using transformation (28) and (42)–(43). In addition, fields can be obtained at the cell's boundaries at the time moments $n-1/2,n+1/2,\cdots$, by exploiting (38). Therefore, output and the excitation in the GSCN can be taken/applied both at the cell's center and at the cell's boundaries.

The derivation of the GSCN opens up the prospect of developing new nodes with hitherto unexplored combinations of link and stub parameters. Obviously, the node without stubs,

the SSCN, requires the least computer storage and is the most efficient but its implementation is more complicated due to the presence of link lines with different impedances. The only reason why one should combine the complexity of such a scheme with the extra storage of stubs is to achieve better propagation characteristics. The possibilities opened up by the GSCN formulation have been exploited to develop and implement the matched SCN (MSCN) [23] and the adaptable SCN (ASCN) [24]. These nodes use combinations of link and stub parameters which offer improved accuracy and minimized dispersion error in modeling inhomogeneous microwave circuits [23], [24].

REFERENCES

[1] P. B. Johns, "A symmetrical condensed node for the TLM method," *IEEE Trans. Microwave Theory Tech.*, vol. MTT-35, no. 4, pp. 370–377, Apr. 1987.

[2] R. A. Scaramuzza and A. J. Lowery, "Hybrid symmetrical condensed node for TLM method," *Electron. Lett.*, vol. 26, no. 23, pp. 1947–1949, Nov. 1990.

[3] P. Berrini and K. Wu, "A pair of hybrid symmetrical condensed TLM nodes," *IEEE Microwave Guided Wave Lett.*, vol. 4, no. 7, pp. 244–246, July 1994.

[4] V. Trenkic, C. Christopoulos, and T. M. Benson, "New symmetrical super-condensed node for the TLM method," *Electron. Lett.*, vol. 30, no. 4, pp. 329–330, Feb. 1994.

[5] ——, "Generally graded TLM mesh using the symmetrical super-condensed node," *Electron. Lett.*, vol. 30, no. 10, pp. 795–797, May 1994.

[6] ——, "Theory of the symmetrical super-condensed node for the TLM method," *IEEE Trans. Microwave Theory Tech.*, vol. 43, no. 6, pp. 1342–1348, June 1995.

[7] P. Naylor and R. A. Desai, "New three dimensional symmetrical condensed lossy node for solution of electromagnetic wave problems by TLM," *Electron. Lett.*, vol. 26, no. 7, pp. 492–493, Mar. 1990.

[8] F. J. German, G. K. Gothard, and L. S. Riggs, "Modeling of materials with electric and magnetic losses with the symmetrical condensed TLM method," *Electron. Lett.*, vol. 26, no. 16, pp. 1307–1308, Aug. 1990.

[9] P. Naylor and R. Ait-Sadi, "Simple method for determining 3-D TLM nodal scattering in nonscalar problems," *Electron. Lett.*, vol. 28, no. 25, pp. 2353–2354, Dec. 1992.

[10] V. Trenkic, C. Christopoulos, and T. M. Benson, "Simple and elegant formulation of scattering in TLM nodes," *Electron. Lett.*, vol. 29, no. 18, pp. 1651–1652, Sept. 1993.

[11] Z. Chen, M. N. Ney, and W. J. R. Hoefer, "A new finite-difference time-domain formulation and its equivalence with the TLM symmetrical condensed node," *IEEE Trans. Microwave Theory Tech.*, vol. 39, no. 12, pp. 2160–2169, Dec. 1991.

[12] M. Krumpholz and P. Russer, "A field theoretical derivation of TLM," *IEEE Trans. Microwave Theory Tech.*, vol. 42, no. 9, pp. 1660–1668, Sept. 1994.

[13] H. Jin and R. Vahldieck, "Direct derivations of TLM symmetrical condensed node and hybrid symmetrical condensed node from Maxwell's equations using centered differencing and averaging," *IEEE Trans. Microwave Theory Tech.*, vol. 42, no. 12, pt. 2, pp. 2554–2561, Dec. 1994.

[14] D. A. Al-Mukhtar and J. E. Sitch, "Transmission-line matrix method with irregularly graded space," *IEE Proc.*, pt. H, vol. 128, no. 6, pp. 299–305, Dec. 1981.

[15] C. Christopoulos, *The Transmission-Line Modeling (TLM) Method.* Piscataway, NJ: IEEE Press, 1995.

[16] S. Akhtarzad and P. B. Johns, "Generalized elements for TLM method of numerical analysis," *Proc. IEE*, vol. 122, no. 12, pp. 1349–1352, Dec. 1975.

[17] P. P. M. So and W. J. R. Hoefer, "A new look at the 3D condensed node TLM scattering," in *IEEE Int. Microwave Symp. Dig.*, Atlanta, Ga, June 1993, pp. 1443–1446.

[18] V. Trenkic, T. M. Benson, and C. Christopoulos, "Dispersion analysis of a TLM mesh using a new scattering matrix formulation," *IEEE Microwave Guided Wave Lett.*, vol. 5, no. 3, pp. 79–80, Mar. 1995.

[19] R. E. Collin, *Foundations for Microwave Engineering*, 2nd ed. New York: McGraw-Hill, 1992.

[20] D. P. Johns, "An improved node for frequency-domain TLM—The 'Distributed Node'," *Electron. Lett.*, vol. 30, no. 6, pp. 500–502, Mar. 1994.

[21] P. Berrini and K. Wu, "A new frequency domain symmetrical condensed TLM node," *IEEE Microwave Guided Wave Lett.*, vol. 4, no. 6, pp. 180–182, June 1994.

[22] J. L. Herring and C. Christopoulos, "The application of different meshing techniques to EMC problems," in *9th Annu. Rev. Prog. in Applied Comp. in EM*, NPS Monterey, CA, 1993, pp. 755–762.

[23] V. Trenkic, C. Christopoulos, and T. M. Benson, "Advanced node formulations in TLM—The matched symmetrical condensed node (MSCN)," in *Proc. 12th Annu. Rev. Prog. in Applied Comp. Electromagn.*, Monterey, CA, Mar. 18–22, 1996, vol. 1, pp. 246–253.

[24] ——, "Advanced node formulations in TLM—The adaptable symmetrical condensed node," *IEEE Trans. Microwave Theory Tech.*, vol. 44, no. 12, pt. II, pp. 2473-2478, Dec. 1996.

Vladica Trenkic (M'96) was born in Aleksinac, Yugoslavia, in 1968. He received the Dipl.Ing. degree in electrical engineering with computer science from the University of Niš, Niš, Yugoslavia, in 1992 and the Ph.D. degree from the University of Nottingham, Nottingham, U.K., in 1995.

Since 1992, he has been a Research Assistant, Department of Electrical and Electronic Engineering, University of Nottingham. His research interests include numerical modeling using the transmission line modeling method and its implementation to electromagnetic compatibility and microwave heating problems.

Dr. Trenkic received the IEE Electronics Letters Premium award in 1995.

Christos Christopoulos (M'92) was born in Patras, Greece, in 1946. He received the Diploma in electrical and mechanical engineering from the National Technical University of Athens, Athens, Greece, in 1969 and the M.Sc. and D.Phil. degrees from the University of Sussex, Sussex, U.K., in 1970 and 1975, respectively.

In 1974, he joined the Arc Research Project of the University of Liverpool, Liverpool, U.K., and spent two years working on vacuum arcs and breakdown while on attachment to the UKAEA Culham Laboratories. In 1976, he joined the University of Durham, U.K., as a Senior Demonstrator in Electrical Engineering Science. In October 1978, he joined the Department of Electrical and Electronic Engineering, University of Nottingham, Nottingham, U.K., where he is now Professor of Electrical Engineering. His research interests are in electrical discharges and plasmas, electromagnetic compatibility, electromagnetics, and protection and simulation of power networks.

Dr. Christopoulos received the IEE Snell Premium and IEE Electronics Letters Premium awards in 1995.

Trevor M. Benson (M'96) was born in 1958. He received the first-class honors degree in physics and the Clark Prize in experimental physics from the University of Sheffield, Sheffield, U.K., in 1979 and the Ph.D. degree from the same university in 1982.

After spending over six years as a Lecturer at University College, Cardiff, Wales, he joined the University of Nottingham, Nottingham, U.K., as a Senior Lecturer in Electrical and Electronic Engineering in 1989, was promoted to the post of Reader in 1994, and Professor of Optoelectronics in 1996. His current research interests include experimental and numerical studies of electromagnetic fields and waves with particular emphasis on propagation in optical waveguides and electromagnetic compatibility.

Dr. Benson received the IEE Electronics Letters Premium Award in 1995.